Properties of Cage Rearrangements Observed near the Colloidal Glass Transition

Eric R. Weeks*
Physics Department, Emory University, Atlanta, Georgia 30322

D. A. Weitz
Department of Physics and DEAS, Harvard University, Cambridge, Massachusetts 02138
(Received 12 July 2001; published 12 August 2002)

We use confocal microscopy to study particle motion in colloidal systems. Near the glass transition, motion is inhibited, as particles spend time trapped in transient "cages" formed by neighboring particles. We measure the cage sizes and lifetimes, which, respectively, shrink and grow as the glass transition approaches. Cage rearrangements are more prevalent in regions with lower concentrations and higher disorder. Neighboring rearranging particles typically move in parallel directions, although a nontrivial fraction moves in antiparallel directions, usually from particle pairs with initial separations corresponding to local maxima and minima of the pair correlation function $g(r)$, respectively.

DOI: 10.1103/PhysRevLett.89.095704 PACS numbers: 64.70.Pf, 61.20.Ne, 61.43.Fs, 82.70.Dd

Many liquids undergo a glass transition when rapidly cooled, where their viscosity grows by orders of magnitude for only modest decreases in temperature. This drastic increase in viscosity is unaccompanied by significant structural changes; instead, the dynamics slow dramatically. Physically, this slowing of the dynamics reflects the confinement of any given particle by a "cage" formed by its neighbors; it is the rearrangement of the cage which leads to the final structural relaxation, allowing the particle to diffuse through the sample [1]. The dynamics of cages have been studied with scattering measurements, which probe a spatial and temporal average of their behavior, and with computer simulations; however, in real systems, the actual motion of the individual particles involved in cage dynamics and breakup are still poorly understood [1–9].

In this paper, we study the motion of the individual particles and their neighbors during cage breakup, and provide the first direct experimental visualization of this process. We use confocal microscopy to study the motion of colloidal particles in a dense suspension, an excellent model for the glass transition [10–12]. The rearrangement of cages involves the cooperative motion of neighboring particles [2–7], for example, as shown in Fig. 1, where the most mobile particles have arrows indicating the direction of their motion. While most neighboring particles move in similar directions, a significant minority move in opposite directions, resulting in local changes in topology. We also find that the more mobile particles are located in regions with a lower local volume fraction, and higher disorder. These measurements provide a direct, quantitative physical picture of the nature of cage rearrangements.

We use sterically stabilized poly-(methylmethacrylate) particles with a radius $a = 1.18\ \mu$m [3,10,13], immersed in a mixture of decalin and cycloheptylbromide. This solvent simultaneously matches the particle index of refraction and density to mitigate the effects of scattering and sedimentation. Hard sphere particles undergo a freezing transition at a volume fraction $\phi_f = 0.494$, a melting transition at $\phi_m = 0.545$, and have a glass transition at $\phi_g \approx 0.58$. [10,12]. To visualize the particles, we stain them with fluorescent rhodamine dye; this imparts a slight charge to the particles, shifting the phase transition boundaries to $\phi_f \approx 0.38$, $\phi_m \approx 0.42$, and $\phi_g \approx 0.58$. We image a volume 60 μm $\times$ 60 μm $\times$ 10 μm, containing several thousand particles, and identify particle centers with an accuracy of at least 0.05 μm [13]. A typical particle trajectory is shown in the inset of Fig. 1; it exhibits caged motion, with a sudden cage rearrangement which lasts $\sim$600 s.

The effect of cages on the ensemble dynamics [1–9,12] is evident from the particle mean square displacement, $\langle \Delta x^2 \rangle$, shown in Fig. 2(a) for three supercooled colloidal fluids ($\phi < \phi_g$). At the earliest times, particle motion is diffusive, as they have not moved far enough to encounter the cage formed by their neighbors. As their displacement

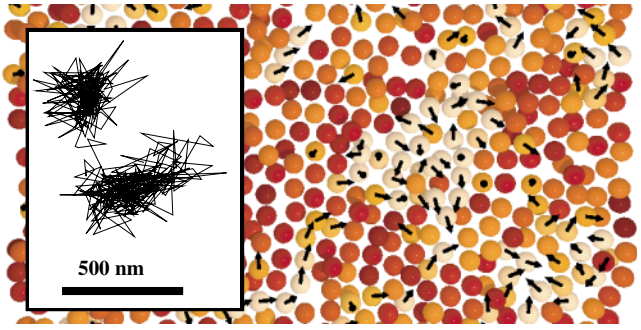

FIG. 1 (color). A cut through a three-dimensional sample, with arrows indicating the direction of motion for particles with displacements $\Delta r > 0.2\ \mu$m, using $\Delta t^* = 600$ s. The sample has $\phi = 0.52$, and the cut is 2.5 μm thick ($\sim$1 layer of particles). The arrows are all the same length in three dimensions, so shortened arrows indicate motion in or out of the picture. Lighter colors indicate particles with larger displacements. Inset: 120 min trajectory of one particle from this sample.

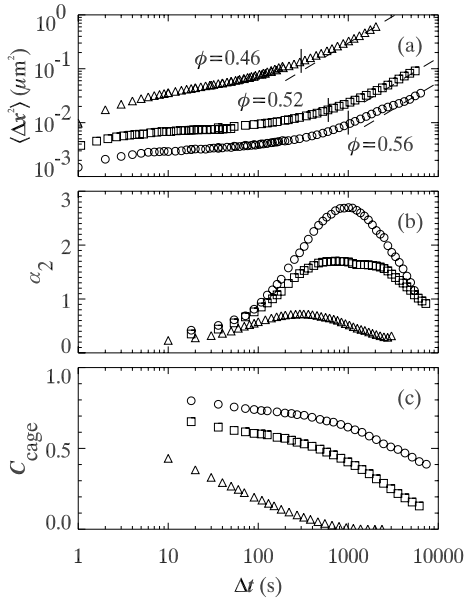

FIG. 2. (a) Mean square displacements. The diagonal straight lines indicate estimates for $\langle \Delta x^2 \rangle \sim 2D_\infty \Delta t$. Vertical bars indicate Δt^*. $\langle \Delta x^2 \rangle$ is shown rather than $\langle \Delta r^2 \rangle$ as the poorer z resolution artificially increases $\langle \Delta r^2 \rangle$. (b) Non-Gaussian parameter $\alpha_2(\Delta t)$. (c) The cage correlation function.

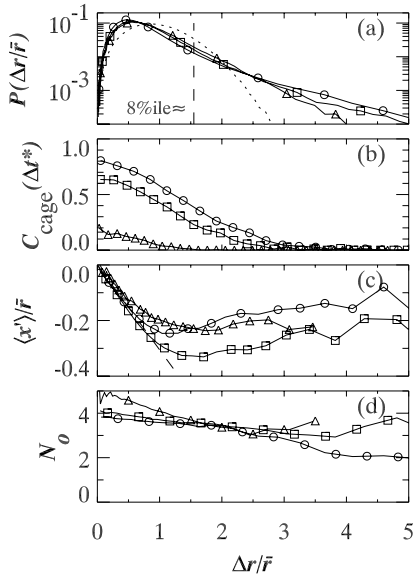

FIG. 3. (a) Step-size distribution. The vertical dashed line indicates the 8% cutoff. The dotted line is a Gaussian with width $\bar{r} = 1$. (b) $C_{\rm cage}(\Delta t^*; \Delta r)$. (c) Average subsequent displacement $\langle x' \rangle$ along the direction of the original displacement Δr. The dashed line is a linear fit to the small Δr region for $\phi = 0.56$ (circles). (d) The average number of ordered neighbors N_o particles have. The symbols are: triangles $\phi = 0.46$, $\Delta t^* = 300$ s, $\bar{r} = 0.61\,\mu$m; squares $\phi = 0.52$, $\Delta t^* = 600$ s, $\bar{r} = 0.22\,\mu$m; circles $\phi = 0.56$, $\Delta t^* = 1000$ s, $\bar{r} = 0.16\,\mu$m.

becomes larger, their motion is impeded by the cage, leading to the plateau in $\langle \Delta x^2 \rangle$. The displacement at the plateau decreases as ϕ increases, reflecting the smaller cage size. Moreover, the cages become more long-lived with increasing ϕ, presumably because cage rearrangements involve a larger number of particles as the glass transition is approached [2–7]. Cage rearrangement leads to an upturn in $\langle \Delta x^2 \rangle$ at the end of the plateau; at even longer lag times, the motion again becomes diffusive, albeit with a greatly decreased diffusion coefficient, D_∞, as indicated by the dashed lines in Fig. 2(a).

We estimate the cage rearrangement time scale, Δt^*, by finding the maximum of the non-Gaussian parameter $\alpha_2(\Delta t) = \langle \Delta x^4 \rangle / (3\langle \Delta x^2 \rangle^2) - 1$, shown in Fig. 2(b). α_2 is computed from the 1D displacement distribution $P(\Delta x; \Delta t)$ [3–6], and is zero for a Gaussian distribution, and largest when there are broad tails. To compare these distributions for different ϕ, we normalize the displacements Δr by the average, $\bar{r} \equiv \langle \Delta r^2 \rangle^{1/2}$. The radial step-size distribution $P(\Delta r/\bar{r}; \Delta t^*)$ is plotted for three values of ϕ in Fig. 3(a). There are more large displacements than expected for a Gaussian distribution, shown by the dashed line, reflecting the anomalously large motion of the particles undergoing cage rearrangements.

These large displacements contribute to the increase in the mean square displacement at lag times greater than Δt^*. To confirm that this motion directly reflects structural relaxation, we calculate a topological cage correlation function, $C_{\rm cage}(\Delta t)$ [8]. We define particles as nearest neighbors if their separation is less than a cutoff distance set by the first minimum of $g(r)$; $C_{\rm cage}(\Delta t)$ is the fraction of particles with the same neighbors at time t and time $t + \Delta t$, averaged over all t. As shown in Fig. 2(c), for the lowest volume fraction, $\phi = 0.46$ (triangles), particles are barely caged, but as ϕ increases toward ϕ_g, the decay of $C_{\rm cage}$ slows dramatically. To determine which particles are responsible for topological changes, we replot $C_{\rm cage}(\Delta t^*)$ as a function of the normalized displacement; in this case the average is over all particles with a given normalized displacement. As shown in Fig. 3(b), $C_{\rm cage}(\Delta t^*)$ decreases significantly for particles with larger displacements, confirming that these contribute most to the structural relaxation.

To directly measure the cage size, we investigate the temporal correlations of the motion of individual particles [9]. Caged particles must have no significant net displacement over long times; by contrast particles whose cages rearrange do have net displacements. To quantify this, we compare a particle's displacements $\Delta\vec{r}$ and $\Delta\vec{r}'$ during sequential time intervals of Δt^*. We focus on x', the component of $\Delta\vec{r}'$ along the direction of the original displacement $\Delta\vec{r}$; $\langle x' \rangle$ is plotted in Fig. 3(c). $\langle x' \rangle$ is always less than zero, indicating that the average motion is anticorrelated. For small initial displacements the behavior is linear, $x' = -c|\langle \Delta\vec{r} \rangle|$. Cages constrain particles so that the farther a particle moves, the farther it moves back: large values of c indicate highly anticorrelated motion, with c having a

maximum possible value of 1/2 for a cage with perfectly rigid walls [9]. The linear relationship fails for larger displacements, as seen in Fig. 3(c); particles move shorter distances $\langle x' \rangle$ than expected by extrapolation from the small $\Delta\vec{r}$ behavior. We identify the end of the linear regime as the cage size, r_{cage} [9]. For comparison, we estimate the size of the cage by other methods. The simplest is the free volume of the system compared to random close packing, $r_{\text{free}} = 4a[(\phi_{rcp}/\phi)^{1/3} - 1]$. Another estimate comes from the mean square displacement at the cage rearrangement time scale Δt^*, $r_{\text{msd}} = \langle \Delta r^2(\Delta t^*) \rangle^{1/2}$. The final estimate is $\Delta r^*(\Delta t^*)$, chosen so that 5% of particles have displacements $\Delta r > \Delta r^*$ [3,6]. The estimated values are listed in Table I and are in good agreement. The cage size decreases as ϕ_g is approached [9,14], accounting for the increase in $C_{\text{cage}}(\Delta t^*)$ seen in Fig. 2(c): particles undergoing cage rearrangements move shorter distances, and thus their topology changes less.

We can use this cage size to model the particle motion as a random walk, alternating between steps (cage rearrangements) and pauses (caging). Each individual step is not random, but is due to the motion of a particle of a distance $\sim r_{\text{cage}}$. From the central limit theorem, $D_\infty = r_{\text{cage}}^2/2\Delta t^{**}$, where Δt^{**} is the mean time between steps, or the average cage lifetime [15]. The estimated values of D_∞, and the values calculated for Δt^{**} are listed in Table I. We find that Δt^{**} is significantly larger than Δt^*, the time scale for a particle to move *during* one cage rearrangement. Both grow as ϕ increases, consistent with previous experiments [1,11,12] and simulations [4–9,14]. While the cage size decreases, it remains finite as ϕ_g is approached, implying that the dramatic decrease in D_∞ is due primarily to the increasing cage lifetime. The α-relaxation time scales with Δt^{**}; τ_α is the time scale for which all of the particles have diffused roughly the interparticle spacing, thus $\tau_\alpha/\Delta t^{**} \approx (2a/r_{\text{cage}})^2$ [1]. Our random-walk picture also yields an unambiguous estimate of the fraction of particles involved in cage rearrangements at any given time; it is given by the ratio $\Delta t^*/\Delta t^{**}$. This ratio is $\sim$8% for all samples except the most dilute (for which it is 16%); it is shown by the vertical dashed line in Fig. 3(a).

Several computer simulations looked for the underlying origins of cage rearrangements, and found correlations between mobile particles and their local environments [6,7,16,17]. Mobile particles tended to be in regions with higher disorder [7,16,17], lower density [7,17], and higher potential energy (and thus higher disorder) [6]. Ultimately, our samples crystallize, and it is possible that the evolution to crystalline order drives the structural relaxation. To investigate this possibility, we quantify the local order with an order parameter that identifies local crystalline regions [18]. If two adjacent particles have similar orientations of their neighbors the two particles are ordered neighbors; most particles have between two and four ordered neighbors. Particles with larger displacements have fewer ordered neighbors, as shown in Fig. 3(d), in agreement with the correlation between mobility and disorder seen in simulations [6,7,16,17]. Furthermore, the mobile colloidal particles typically move to positions where their number of ordered neighbors has increased by $\sim$1, suggesting a slow evolution toward crystalline structure. Thus, any effect of the local crystal order on the cage rearrangement may be driven more by local variations in ϕ, rather than an evolution to the state with the lowest global energy minimum [18]. In fact, we find that the volumes of the Voronoi polyhedra associated with the mobile particles are larger on average, giving a local volume fraction as much as $\delta\phi = O(0.03)$ lower than the mean. This suggests that the particles with smaller ϕ are farther from ϕ_g and thus are more likely to rearrange, in agreement with the simulations [6,7,17]. The Voronoi volume varies from particle to particle; the correlation between mobility and local volume is only an average tendency.

Cage rearrangement is not strictly a localized event; instead, many neighboring particles are typically involved, often moving in similar directions, as shown by Fig. 1 [2–7]. To quantify the propensity for motion of neighboring particles in the same direction, we calculate the distribution of angles, $P(\theta)$, between the displacement vectors of all neighboring particles, measured at Δt^* to define the displacements. The probability of observing two displacement vectors forming an angle in the range $(\theta, \theta + d\theta; \phi, \phi + d\phi)$ is given by $P(\theta, \phi)\sin\theta\, d\theta\, d\phi$; in Fig. 4(a) we plot $P(\theta, \phi)$ which, by symmetry, depends only on θ. This function is strongly peaked at $\theta \approx 0$, indicating that two particles usually move in parallel directions, sometimes termed ''strings,'' but also including three-dimensional groups of particles moving in parallel directions [3,5–7]. However, a significant fraction of particles move in antiparallel directions ($\theta \approx \pi$), which we

TABLE I. Estimates for the cage size, the cage rearrangement time scale Δt^*, the cage lifetime Δt^{**}, and the estimated asymptotic diffusion coefficient D_∞.

	Cage size (μm)				Time scales (hr)		
ϕ	r_{cage}	r_{free}	r_{msd}	Δr^*	Δt^*	Δt^{**}	D_∞ (μm^2/s)
0.46	0.75	0.55	0.63	1.12	0.083	0.52	$15 \cdot 10^{-5}$
0.52	0.35	0.35	0.23	0.40	0.17	2.1	$0.80 \cdot 10^{-5}$
0.53	0.45	0.31	0.27	0.49	0.67	9.4	$0.30 \cdot 10^{-5}$
0.56	0.25	0.21	0.17	0.29	0.28	3.3	$0.26 \cdot 10^{-5}$

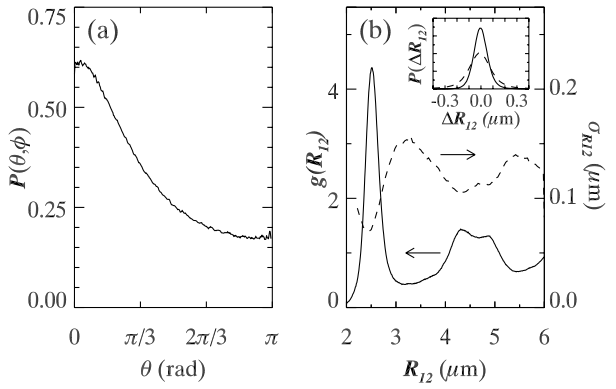

FIG. 4. (a) Probability distribution of angle between displacement vectors for two neighboring particles, as a function of the polar angle θ. (b) Pair correlation function $g(R_{12})$ (solid line) and width σ_{R12} of probability distribution function $P(\Delta R_{12}|R_{12})$ (dashed line). The inset shows $P(\Delta R_{12}|R_{12})$ for nearest neighbors, with initial separations of 2.4 μm $< R_{12} <$ 2.6 μm (solid line), and antineighbors with 3.0 μm $< R_{12} <$ 3.2 μm (dashed line). All data are for $\phi = 0.56$ and $\Delta t^* = 1000$ s.

term ''mixing regions.'' When $\theta \approx \pi$, particles are either converging or diverging; examples of each case can be seen in Fig. 1. We find that these ''mixing'' pairs of particles ($\theta > \pi/2$) are approximately twice as likely to result in the two particles no longer being neighbors (compared to the pairs with with $\theta < \pi/2$). Thus, these rearrangements, while less frequent, are responsible for much of the topological changes.

To investigate the nature of the correlated motion of neighboring particles, we calculate the probability distribution function, $P(\Delta R_{12}|R_{12})$, which measures the change in separation, ΔR_{12}, between two nearby particles, initially separated by R_{12}, after a time interval Δt^*. These distributions are narrower if R_{12} corresponds to a peak of the pair correlation function, $g(R_{12})$, than if R_{12} corresponds to a minimum, as shown by the solid and dashed lines in the inset of Fig. 4(b), respectively. This is shown more dramatically in Fig. 4(b), where we compare the widths of the distribution functions, $\sigma_{R_{12}}$, directly with $g(R_{12})$, showing that they are anticorrelated. This is reminiscent of the behavior of the collective diffusion coefficient, which varies as the inverse of the static structure factor, $D(q) \sim 1/S(q)$ [19]. The relaxation of fluctuations at the peak of the structure factor, which reflects the most favorable structure, is slowed relative to other values of q. Our results show a similar behavior occurs in real space; particles whose separation corresponds to a peak in $g(R_{12})$ are in more favorable relative positions and tend to move together, so that their separation does not change; by contrast, particles whose separation corresponds to minima of $g(R_{12})$ are in less favorable relative positions, and tend to move in antiparallel directions.

This work reveals a physical picture of cage trapping and rearrangement. Cage rearrangements involve localized clusters of particles with large displacements, in regions with higher disorder and higher free volume. Both the collective nature of the relaxation, and the local origin of the cage rearrangements, clearly play a key role in the behavior of supercooled fluids of colloidal suspensions; it remains to be seen whether they also are important effects in other glasses.

We thank J. Conrad, J. C. Crocker, B. Doliwa, U. Gasser, S. C. Glotzer, H. Gould, and K. Vollmayr-Lee for helpful discussions. We thank A. Schofield for providing our colloidal samples. This work was supported by NSF (DMR-9971432) and NASA (NAG3-2284).

*Electronic address: weeks@physics.emory.edu

[1] M. D. Ediger, C. A. Angell, S. R. Nagel, J. Phys. Chem. **100**, 13 200 (1996); C. A. Angell, J. Phys. Condens. Matter **12**, 6463 (2000).
[2] W. K. Kegel and A. van Blaaderen, Science **287**, 290 (2000).
[3] E. R. Weeks, J. C. Crocker, A. C. Levitt, A. Schofield, and D. A. Weitz, Science **287**, 627 (2000).
[4] W. Kob, C. Donati, S. J. Plimpton, P. H. Poole, S. C. Glotzer, Phys. Rev. Lett. **79**, 2827 (1997).
[5] C. Donati *et al.*, Phys. Rev. Lett. **80**, 2338 (1998).
[6] C. Donati, S. C. Glotzer, P. H. Poole, W. Kob, and S. J. Plimpton, Phys. Rev. E **60**, 3107 (1999).
[7] D. N. Perera and P. Harrowell, J. Chem. Phys. **111**, 5441 (1999).
[8] E. Rabani, J. D. Gezelter, and B. J. Berne, J. Chem. Phys. **107**, 6867 (1997).
[9] B. Doliwa and A. Heuer, Phys. Rev. Lett. **80**, 4915 (1998).
[10] P. N. Pusey and W. van Megen, Nature (London) **320**, 340 (1986).
[11] E. Bartsch, V. Frenz, S. Möller, and H. Silescu, Physica (Amsterdam) **201A** , 363 (1993).
[12] W. van Megen and S. M. Underwood, Phys. Rev. E **49**, 4206 (1994).
[13] A. D. Dinsmore, E. R. Weeks, V. Prasad, A. C. Levitt, and D. A. Weitz, Appl. Opt. **40**, 4152 (2001).
[14] P. Allegrini, J. F. Douglas, and S. C. Glotzer, Phys. Rev. E **60**, 5714 (1999).
[15] E. R. Weeks and H. L. Swinney, Phys. Rev. E **57**, 4915 (1998).
[16] H. Yin and B. Chakraborty, Phys. Rev. Lett. 86, 2058 (2001).
[17] V. A. Luchnikov, N. N. Medvedev, Yu. I. Naberukhin, V. N. Novikov, Phys. Rev. B **51**, 15 569 (1995).
[18] P. Rein ten Wolde, M. J. Ruiz-Montero, and D. Frenkel, J. Chem. Phys. **104**, 9932 (1996); U. Gasser, E. R. Weeks, A. Schofield, P. N. Pusey, and D. A. Weitz, Science **292**, 258 (2001).
[19] P. N. Pusey, in *Liquids, Freezing and the Glass Transition*, edited by J. P. Hansen, D. Levesque, and J. Zinn-Justin (Elsevier, Amsterdam, 1991), Chap. 10.